JOURNAL OF PETROLOGY | VOLUME 41 | NUMBER 12 | PAGES 1653–1671 | 2000

The Archaean High-Mg Diorite Suite: Links to Tonalite–Trondhjemite–Granodiorite Magmatism and Implications for Early Archaean Crustal Growth

R. H. SMITHIES[1]* AND D. C. CHAMPION[2]

[1]GEOLOGICAL SURVEY OF WESTERN AUSTRALIA, 100 PLAIN STREET, EAST PERTH, WA 6004, AUSTRALIA

[2]AUSTRALIAN GEOLOGICAL SURVEY ORGANISATION, GPO BOX 378, CANBERRA, ACT 2601, AUSTRALIA

RECEIVED MAY 14, 1999; REVISED TYPESCRIPT ACCEPTED APRIL 17, 2000

The 2·95 Ga Pilbara high-Mg diorite suite intrudes the central part of the Archaean granite–greenstone terrain of the Pilbara Craton, Western Australia, and shows many features typical of high-Mg diorite (sanukitoid) suites from other late Archaean terrains. Such suites form a minor component of Archaean felsic crust. They are typically emplaced in late- to post-kinematic settings, sometimes in association with felsic alkaline magmatism, and are either unaccompanied by, or post-date, tonalite–trondhjemite–granodiorite (TTG) magmatism, which comprises a much greater proportion of Archaean felsic crust. The TTG series comprises sodic, Sr-rich rocks with high La/Yb and Sr/Y ratios, thought to result from partial melting of eclogite facies basaltic crust. High-Mg diorite shares these characteristics but has significantly higher mg*-number (~ 60), and Cr and Ni concentrations, suggesting a mantle source. Many compositional features of TTGs are also shared by Cenozoic felsic magmas called adakites. Adakites form by melting of a young, hot, subducting slab and provide an* a priori *reason to invoke a subduction origin for TTG. During ascent through the mantle wedge, adakite commonly assimilates, or is contaminated by, peridotite, and the resulting 'wedge-modified adakite' bears strong compositional similarity to Archaean high-Mg diorite. Nevertheless, the latter are not simply an Archaean analogue of 'wedge-modified adakite' (i.e. 'wedge-modified TTG') because their intrusion is post-tectonic and unaccompanied by TTG magmatism. The petrogenesis of the Pilbara high-Mg diorite suite requires remelting of a mantle source, extensively metasomatized by addition of about 40% TTG-like melt. However, although the generation of this metasomatized source appears to require a subduction environment, many Archaean TTG suites show no clear chemical evidence of having interacted with a mantle wedge, and on that basis are more likely to represent partial melts of basaltic lower crust rather than of subducted slab. High-Mg diorite suites appear to concentrate in the Late Archaean, suggesting that subduction may have become an important process only after ~ 3·0 Ga.*

KEY WORDS: *Archaean; high-Mg diorite; sanukitoid; TTG; adakite; crustal evolution; Pilbara Craton*

INTRODUCTION

The sodic and calcic granitoids that form a large proportion of many Archaean terrains can be subdivided into the tonalite–trondhjemite–granodiorite (TTG) series and the high-Mg diorite (or sanukitoid) suite. The TTG series represents, by far, the greater volume. These siliceous (SiO_2 ~70 wt %) and aluminous (Al_2O_3 >15%) rocks, with low Yb (<1 ppm), high La/Yb (generally >30), Na_2O/K_2O (>1) and Sr and Ba (both >500 ppm) (Barker & Arth, 1976; Barker, 1979) (Table 1), are considered to be the result of partial melting of eclogite facies basaltic crust (e.g. Arth & Hanson, 1975; Barker

*Corresponding author. e-mail: r.smithies@dme.wa.gov.au

Published by Oxford University Press 2000

& Arth, 1976; Barker, 1979; Tarney *et al.*, 1979; Martin, 1986; Drummond & Defant, 1990; Rapp *et al.*, 1991; Rapp, 1997). The major and trace element compositions of TTG are very similar to those of Cenozoic adakite (Table 1), which is thought to be restricted to zones where young, hot, oceanic crust is subducted and partially melted at pressures high enough to stabilize garnet ± amphibole (e.g. Defant & Drummond, 1990), and accordingly it has been suggested that TTG is the Archaean, subduction related, analogue of adakite (e.g. Drummond & Defant, 1990; Drummond *et al.*, 1996; Martin, 1999).

In contrast to TTG, rocks of the high-Mg diorite suite generally range in composition from diorite to granodiorite and are characterized by significantly higher *mg*-number [$= Mg^{2+}/(Mg^{2+} + Fe_{Total}) \times 100$, with Fe_{Total} as Fe^{2+}], Cr, Ni and large-ion-lithophile element (LILE) contents (Table 1) (Shirey & Hanson, 1984; Stern *et al.*, 1989). At about 60 wt % SiO_2, high-Mg diorite has *mg*-number ~60, Cr ~200 ppm and Ni ~100 ppm, requiring a source significantly more mafic than typical Archaean basaltic crust; that is, a mantle source. High-Mg diorite magmatism was first documented from the Superior Province of North America (Shirey & Hanson, 1984) and is generally regarded only as a minor, though widespread, component of that province (Beakhouse *et al.*, 1999) and other Archaean terrains. Nevertheless, high-Mg diorite is the only Archaean felsic magma type that appears to be derived from the mantle, and an understanding of its petrogenesis, tectonic setting and possible relationship to the more voluminous TTG series may provide a better understanding of Archaean crustal evolution.

The major element geochemistry of high-Mg diorite resembles that of Miocene high-Mg andesite (sanukite) from the Setouchi volcanic belt of Japan (Shirey & Hanson, 1984) (Table 1). Tatsumi & Ishizaka (1982) suggested that sanukite results from the partial melting of hydrous mantle peridotite, and Shirey & Hanson (1984) argued for a similar origin for Archaean high-Mg diorite. However, high-Mg diorite has much higher La/Yb ratios and Sr and Ba concentrations than sanukite, and in these respects more closely resembles adakite that has been extensively contaminated by mantle peridotite (e.g. Kelemen, 1995; Yogodzinski *et al.*, 1995; Rapp *et al.*, 1999). Adakite melt rising off a subducting slab interacts with the mantle wedge, to produce rocks with significantly lower SiO_2 and higher *mg*-number, Cr and Ni concentrations [e.g. Adak-type high-Mg andesite of Yogodzinski *et al.* (1995) or the high-Mg adakite of Rapp *et al.* (1999)] (Table 1). These Mg-rich rocks will be referred to here as 'wedge-modified adakite'.

The close compositional similarities between high-Mg diorite and wedge-modified adakite suggest a similar origin (e.g. Yogodzinski *et al.*, 1995; Drummond *et al.*, 1996), through mantle contamination of a slab-derived melt. Intrusion of high-Mg diorite, however, is late- to post-kinematic (e.g. Shirey & Hanson, 1984; Stern *et al.*, 1989; Evans & Hanson, 1997; Beakhouse *et al.*, 1999), and is not associated with voluminous magmas commonly interpreted as slab derived, such as adakite or TTG. In this respect its tectonic association differs markedly from that of wedge-modified adakite.

Petrological and geochemical data are presented for a newly discovered, ~2950 Ma, high-Mg diorite suite from the Archaean granite–greenstone terrain of the Pilbara Craton, Western Australia (Fig. 1). These rocks are post-kinematic, or anorogenic, intrusions into an ensialic setting and so their origin cannot be directly linked to contemporaneous subduction. They intrude the youngest supracrustal sequences of the central part of that terrain, and are associated with intrusion of alkaline magmas, but not with TTG.

We develop a two-stage model similar to the one that Evans & Hanson (1997) proposed for the high-Mg diorites of the Superior Province. In our model, the Pilbara high-Mg diorite suite results from the remelting of a mantle source region, previously hybridized by the addition of significant amounts of a slab-derived melt. However, we also show that a subducted slab is not the most likely source of voluminous Archaean TTG suites. The compositional range for many TTG suites, and certainly most TTG from the Pilbara Craton, overlaps only the low *mg*-number, high SiO_2 end of the spectrum of adakite and wedge-modified adakite, and as such, shows little, if any, evidence of having passed through a peridotitic mantle wedge. Melting of hydrated basaltic material at the base of thickened crust (e.g. Atherton & Petford, 1993; Petford & Atherton, 1996), rather than a subducting slab, may be a more appropriate model for most TTG. Because melt produced in this way has limited access to mantle peridotite, it cannot be the precursor to high-Mg diorite. The suggestion that subduction-derived TTG suites are rare may explain why high-Mg diorite suites are also rare, as modification of a mantle source by subduction-derived TTG appears to be a necessary precursor to high-Mg diorite magmatism. These apparent constraints are incorporated into two alternative tectonic scenarios for the evolution of the Archaean felsic crust.

REGIONAL GEOLOGY

The Pilbara Craton lies in the northwest of Western Australia and contains well-exposed middle to late Archaean granite–greenstone terrains, overlain to the south by the little-deformed late Archaean to early Proterozoic volcano-sedimentary sequences of the Hamersley Supergroup (Fig. 1). The eastern part of the granite–greenstone terrain consists of large, ovoid, granitic complexes mantled by belts of tightly folded low-grade,

Table 1: Representative analyses of high-Mg diorite, high-Mg andesite and adakite (including wedge-modified adakite)

	1 Superior Av. 1	2 Superior Av. 2	3 Pilbara 142347	4 Pilbara 142260	5 Setouchi TGI-6	6 Piip-type 35G5A	7 Adak-type V3841Y2	8 Adakite Av. 1	9 Adakite Av. 2	10 TTG Av.
wt %										
SiO_2	56·07	57·36	59·33	61·86	57·72	58·00	59·70	67·72	63·89	69·79
TiO_2	0·71	0·60	0·63	0·51	0·43	0·67	0·89	0·36	0·61	0·34
Al_2O_3	14·88	16·32	14·03	14·48	14·78	17·19	15·43	16·44	17·40	15·56
Fe_2O_3*	7·88	6·34	8·38	6·34	6·07	5·33	3·75	2·72	4·68	3·12
MnO	0·12	0·10	0·11	0·08	0·13	0·08	0·04	0·06	0·08	0·05
MgO	6·85	4·61	5·33	4·17	8·95	6·38	4·76	1·06	2·47	1·18
CaO	7·65	6·39	5·49	4·67	6·31	7·12	7·48	3·71	5·23	3·19
Na_2O	4·04	5·25	3·64	3·91	2·62	3·50	3·69	4·38	4·40	4·88
K_2O	2·23	2·02	2·37	1·80	1·36	0·96	2·08	2·27	1·52	1·76
P_2O_5	0·36	0·37	0·43	0·24	0·10	0·14	0·39	0·14	0·19	0·13
mg-no.	63	59	56	57	74	70	72	44	48	43
ppm										
Ba	1214		1012	695	303†	87	320	1087	485	690
Rb	60	34	106	81	60†	9	13	43	30	55
Sr	1229	1371	632	523	235†	384	2366	1123	869	454
Th			13·0	9·3		0·6	2·88	6·5	3·52	6·9
U			3·0	3·3		0·28	0·97	2·5	0·99	1·6
Zr	111	123	145	130				73	117	152
Nb			8·3	5·3	20†			13	8·3	6·4
Y		11	19·8	15·2	15†	18		15	9·5	7·5
Cr	352	150	224	215	513	262	161	9	54	29
Ni	154	55	120	99	181	127	126	3	39	14
La		43·25	61·60	39·70	12·40	6·27	30·30	29·7	17·55	32
Ce	97·00	98·25	130·20	76·70	24·10	15·10	70·90	50·9	34·65	56
Pr		11·50	14·90	8·60						
Nd		49·75	63·70	32·70			39·80	20·7	20·14	21·4
Sm		8·55		5·40	2·53	1·94	6·85	3·20	3·15	3·3
Eu		2·25		1·40	0·65	0·65	1·74	0·95	0·97	0·92
Gd		5·53		4·30				2·20	2·25	2·2
Tb		0·60		0·60	0·40	0·38	0·48	0·25	0·37	0·31
Dy		2·80		2·60	1·50			1·50	1·43	1·16
Ho		0·47		0·50				0·23		
Er		1·14		1·30				0·58	0·76	0·59
Yb	1·60	0·93		1·20	1·50	1·42	0·62	0·46	0·91	0·55
Lu		0·14		0·20		0·20	0·07		0·15	0·12
La/Yb		46·51		33·08	8·27	4·42	48·87	64·57	19·28	58

1, Average of 11 high-Mg diorites from southwestern Superior Province (Stern *et al.*, 1989); 2, average of four high-Mg diorites with SiO_2 <61 wt %, Jackfish Lake Pluton, Superior Province (Sutcliffe *et al.*, 1990); 3, fine-grained melanodiorite from the Peawah Granodiorite (east) of the Pilbara high-Mg diorite suite; 4, fine-grained melanodiorite from the Jones Well Stock of the Pilbara high-Mg diorite suite; 5, typical Miocene sanukite from the Setouchi volcanic belt of Japan (Tatsumi & Ishizaka, 1982); 6, typical Piip-type high-Mg andesite from the Cainozoic Piip Volcano, western Aleutian arc (Yogodzinski *et al.*, 1995); 7, typical Adak-type high-Mg andesite, Cainozoic western Aleutian arc (Kay, 1978; Yogodzinski *et al.*, 1995)—referred to here as 'wedge-modified adakite'; 8, average of five adakites from Defant *et al.* (1991); 9, average of 140 adakites from Drummond *et al.* (1996); 10, average of 355 TTG from Martin (1994). Av., average.
*All Fe as Fe^{3+}.
†LILE concentrations for Setouchi sanukite of similar SiO_2, quoted by Davis *et al.* (1994).

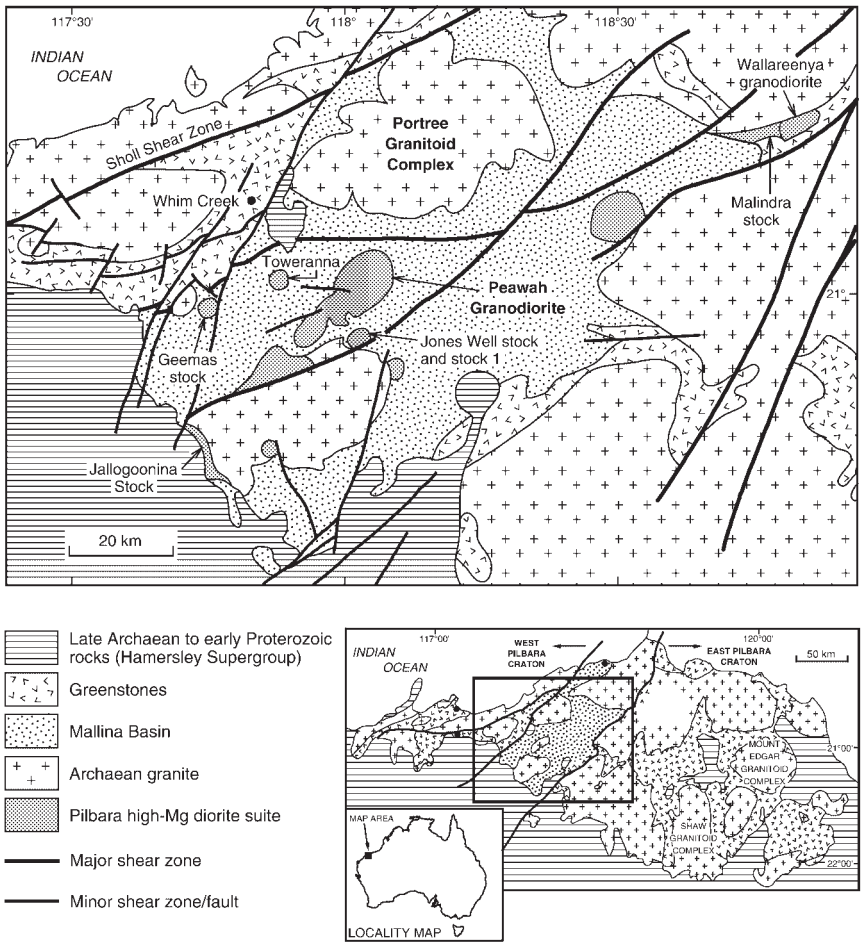

Fig. 1. Regional geological map of the northern part of the Pilbara Craton, showing the Archaean granite–greenstone terrains. Main map shows the Portree Granitoid Complex and the distribution, primarily as intrusions into the rocks of the Mallina Basin, of the Pilbara high-Mg diorite suite.

volcano-sedimentary rocks (greenstones), that accumulated between ~3600 and 2950 Ma. TTG magmatism appears to be predominantly confined to the older (>3440 Ma) portions of the eastern terrain (Champion & Smithies, 1998). In contrast, the western part of the granite–greenstone terrain is characterized by linear, northeast-trending structures and is not known to contain rocks older than ~3270 Ma. In the western terrain, TTG magmatism occurred at ~3260 Ma, 3100–3120 Ma and 2990 Ma.

The rocks of the Pilbara high-Mg diorite suite occur in the central part of the granite–greenstone terrain, where they were intruded into an extensive sequence of deformed turbidites that represent the remnants of the Mallina Basin (Fig. 1). The southeastern margin of this basin is an unconformity or is locally faulted, whereas the present-day margin to the northwest is a fault. The basin is a last stage in the geological evolution of the Pilbara granite–greenstone terrain. Recent geochronological studies (Nelson, 2000) confirm that basin formation occurred after ~3000 Ma (e.g. Smithies *et al.*, 1999). The bulk of the turbidites were folded by ~2950 Ma, at which time they were intruded by the Pilbara high-Mg diorite suite, and by alkaline rocks of the Portree Granitoid Complex (Nelson, 1997, 1999). The rocks of both the high-Mg diorite suite and of the Portree Granitoid Complex are confined to the Mallina Basin, and the intrusions that form the high-Mg diorite suite define a belt that extends for 150 km, parallel to the long axis of that basin (Fig. 1). In the east of the basin, high-Mg diorite was emplaced into zones of active dilation related to extension along major basin-parallel faults (R. H. Smithies, unpublished data, 1999). Thus, emplacement of the suite appears to have been controlled by extensional reactivation of structures related to the earlier evolution of the Mallina Basin.

Slightly younger (~2940–2930 Ma: Nelson, 1997, 1998, 1999) K-rich monzogranite and syenogranite intruded during the second major folding event to affect the central part of the granite–greenstone terrain. This magmatism represents recycling of earlier crust (Champion & Smithies, 1998). Intrusion of these K-rich granites was concentrated along the southeastern margin of the Mallina Basin, and systematically decreased in both age and abundance further to the southeast.

Tectonic setting of the high-Mg diorite suite

The Mallina Basin has been interpreted as an ~3000–2950 Ma intracratonic basin (Smithies *et al.*, 1999). The Pilbara high-Mg diorite suite, and the sodic (Na > K) alkali granites of the Portree Granitoid Complex (Smithies & Champion, 1998), are clearly late- to post-kinematic with respect to the first regional deformation of the Mallina Basin and around 10 my older than the second regional deformation (Smithies, 1998). They also post-date voluminous regional felsic magmatism by between 40 and 60 my, including extensive felsic volcanism in the Whim Creek area, along the faulted northwestern margin of the Mallina Basin (Fig. 1), and pre-date voluminous K-rich felsic magmatism by 10–20 my. In summary, intrusion of the Pilbara high-Mg diorite suite

(1) occurs in an intracontinental setting, unassociated with contemporaneous subduction;

(2) occurs along major faults, reactivated under regional extension;

(3) is directly associated with felsic alkaline magmatism;

(4) is late- to post-kinematic with respect to regional deformation;

(5) post-dates known significant felsic magmatism by ~40 my;

(6) precedes widespread potassic magmatism.

AGE, FIELD RELATIONSHIPS AND PETROGRAPHY OF THE PILBARA HIGH-Mg DIORITE SUITE

The Pilbara high-Mg diorite suite ranges from diorite and monzodiorite to tonalite and granodiorite. Most of the intrusions in the suite are stocks of $< \sim 20$ km^2 (Fig. 1). The Peawah Granodiorite is the largest intrusion (Fig. 1), covering an area of ~180 km^2, and is a composite body that can be geochemically subdivided into the Peawah Granodiorite (east) and the Peawah Granodiorite (west). The Peawah Granodiorite (west) has been dated at 2948 ± 5 Ma (U/Pb SHRIMP; Nelson, 1996). The Wallareenya granodiorite and the Geemas stock (Fig. 1) have been dated at 2954 ± 4 Ma and 2945 ± 6 Ma, respectively (U/Pb SHRIMP; Nelson, 2000). These intrusions are coeval with the alkaline rocks of the Portree Granitoid Complex, which have been dated at 2946 ± 6 Ma (U/Pb SHRIMP; Nelson, 1999).

Many of the intrusions are partially surrounded by earlier intrusions of gabbro. Most intrusions also contain abundant rounded enclaves, up to 30 cm in diameter. Most of these are cognate inclusions of diorite and gabbro. Some intrusions preserve a chilled margin of fine-grained melanodiorite, which also occurs in dykes and sills of 1–2 m thickness in country rock. These rapidly cooled rocks are likely to be the least affected by cumulate processes and hence may preserve compositions close to that of a parental magma.

Mesocratic granodiorite is the most common rock type in the suite and ranges in texture from equigranular to seriate to porphyritic, with plagioclase phenocrysts up to 1 cm long. Plagioclase forms a connected framework of euhedral crystals, many of which show well-developed compositional zoning from inner zones of An_{35} to sodic rims of An_{18}. Small sericite- and calcite-altered cores suggest compositions more calcic than An_{35}.

Hornblende is the dominant mafic mineral. Euhedral hornblende forms part of the early crystallizing plagioclase framework. Subhedral to euhedral hornblende forms an intergranular phase or occurs in allotriomorphic-textured mafic clots. Hornblende shows little compositional variation throughout the suite, with *mg*-numbers ranging between 56 and 66. In most granodiorites, hornblende contains cores of diopside ($Wo_{45–47}En_{40–41}Fs_{13–14}$; *mg*-number ~75), variably altered to actinolite. The abundance of these cores indicates the rocks were initially clinopyroxene rich. Biotite mantles hornblende, or forms an anhedral intergranular phase. It is significantly more Fe rich (*mg*-number ~53) than coexisting hornblende. Quartz and minor microcline are intergranular phases. Accessory minerals include magnetite, sphene, apatite and zircon, which are concentrated in hornblende and biotite. Mafic clots, up to 1 cm in diameter, are locally abundant, and contain hornblende with lesser diopside, biotite, plagioclase and magnetite.

Fine-grained melanodiorite forms a chilled margin to some intrusions. It contains 2–4 mm long phenocrysts of euhedral plagioclase (An_{43} cores to rims of An_{21}), diopside ($Wo_{41}En_{42}Fs_{17}$; *mg*-number ~72) and hornblende (*mg*-number = 65) ± orthopyroxene, in a flow-aligned groundmass of plagioclase and hornblende with lesser biotite (*mg*-number = 52), quartz and magnetite. Orthopyroxene occurs as discrete subhedral crystals, as granoblastic clots containing minor diopside and plagioclase, or as anhedral cores in diopside. It shows significant compositional variation, between $Wo_3En_{59}Fs_{38}$ (*mg*-number = 61) and $Wo_3En_{69}Fs_{28}$ (*mg*-number = 71), with bronzite cores ($Wo_2En_{76}Fs_{22}$, *mg*-number = 77) in larger crystals. Analysis of coexisting clinopyroxene and

orthopyroxene give equilibration temperatures of ~1020°C using the pyroxene thermometer of Wells (1977).

GEOCHEMISTRY OF THE PILBARA HIGH-Mg DIORITE SUITE

Analytical procedures

Rock samples were prepared for chemical analysis by jaw crushing 2–5 kg of sample and then grinding a 50–70 g sub-sample in a tungsten carbide ring mill. Abundances of major and trace elements were determined either at the Australian Geological Survey Organisation (AGSO) in Canberra [X-ray fluorescence (XRF) and inductively coupled plasma mass spectrometry (ICP-MS)], or at the Geology Department, Australian National University (ANU) in Canberra (XRF). Major and minor elements (Si, Ti, Al, Fe, Mn, Mg, Ca, Na, K, P and S) were determined, at both AGSO and ANU, by wavelength-dispersive XRF on fused discs using methods similar to those of Norrish & Hutton (1969). Precision for these elements is better than ±1% of the reported values. Loss on ignition (LOI) was determined by gravimetry after combustion at 1100°C. FeO abundances were determined at AGSO by digestion and electrochemical titration using a modified technique based on Shapiro & Brannock (1962). At AGSO, As, Ba, Cr, Cu, Ni, Sc, V, Zn and Zr were determined by wavelength-dispersive XRF on a pressed pellet using methods similar to those described by Norrish & Chappell (1977). A similar technique was utilized for samples analysed at ANU, using wavelength- and energy-dispersive XRF. Selected trace elements (Cs, Ga, Nb, Pb, Rb, Sb, Sn, Sr, Ta, Th, U and Y) and the rare earth elements (REE) were analysed at AGSO by ICP-MS (Perkin Elmer ELAN 6000) using methods similar to those of Eggins *et al.* (1997). Interlaboratory comparisons exhibit good agreement for major elements, typically within 1–5%, but to 20% and greater for low abundance minor elements (e.g. Ti, Mn and P—with a small absolute error of <0·05 wt %). Trace elements typically agree within 10% (Ba, Rb, Sr, La, Ce, Zr, Y, Ga and V) or up to 20% (Pb, Th, U, Nb, Sc, Cr, Ni, Cu and Zn).

Major and trace element compositions

The most mafic rocks of the Pilbara high-Mg diorite suite show many of the characteristics of high-Mg diorite (sanukitoid). According to Shirey & Hanson (1984), Stern *et al.* (1989) and Stern & Hanson (1991), these characteristics include MgO >6 wt %, *mg*-number >60, Ni and Cr each >100 ppm, Sr and Ba each >500 ppm and high Na_2O, K_2O, light REE (LREE) and La/Yb at silica contents of 60 wt % or less (Fig. 2, Tables 1 and 2). Compared with high-Mg diorite suites from the Superior Province, the Pilbara high-Mg diorite suite has higher FeO, Sc and V and generally higher MgO, Cr and Ni, but lower Sr and generally slightly lower *mg*-number and K_2O, at a given silica content.

The rocks of the Pilbara high-Mg diorite suite have silica contents between ~59 and 70 wt % (Fig. 2), with high *mg*-numbers (62–41) that decrease with increasing silica. Most intrusions plot separately on a SiO_2 vs *mg*-number diagram, and the Wallareenya granodiorite has particularly high *mg*-numbers (Fig. 2). The concentrations of Al_2O_3 vary between 13·5 wt % and 16 wt %, whereas the concentrations of Na_2O and K_2O are moderately high (3·5–4·8 wt % and 1·7–3·3 wt %, respectively) and increase with increasing silica. High concentrations of Cr (20–210 ppm), Ni (15–100 ppm) and V (30–110 ppm) are positively correlated with *mg*-number.

Amongst the LILE, the concentrations of Sr and Ba are high (Sr 300–950 ppm; Ba 450–1600 ppm) but show no clear correlation with silica (Fig. 2), *mg*-number, or with each other. Rubidium varies from 70 to 120 ppm, and Rb/Sr ratios range between 0·14 and 0·25. REE patterns are strongly fractionated (Fig. 3) with La/Yb ratios increasing from 22 to 79 with decreasing *mg*-number, primarily through decreases in the concentrations of the heavy rare earth elements (HREE). No Eu anomalies are observed.

For individual intrusions, trends to lower *mg*-number, Cr, Ni, Y and HREE with increasing silica must primarily reflect removal of hornblende ± clinopyroxene, which is consistent with the presence of these minerals as phenocrysts in fine-grained melanodiorite. Plagioclase is also a phenocryst phase in fine-grained melanodiorite, but the lack of Eu anomalies in the more silicic rocks and the poor correlations between the concentrations of Sr and SiO_2 indicate that plagioclase fractionation was not extensive.

Compositional differences between the parental magmas probably relate more to variations in degrees of partial melting and/or, more particularly, in source composition. At similar *mg*-number, individual intrusions show significantly different concentrations of K_2O, SiO_2 and Th (Figs 2 and 4), suggesting that they did not form from a single parental magma.

Comparisons with Archaean TTG series

Rocks of the TTG series are generally restricted to the older (>~3440 Ma) parts of the Edgar and Shaw granitoid complexes in the eastern part of the Pilbara Craton (Fig. 1) (Bickle *et al.*, 1983, 1989, 1993; Collins, 1983, 1993). Whereas high-Mg diorite and TTG have high LILE, rocks of the high-Mg diorite suite can generally be distinguished by their trends to lower silica and

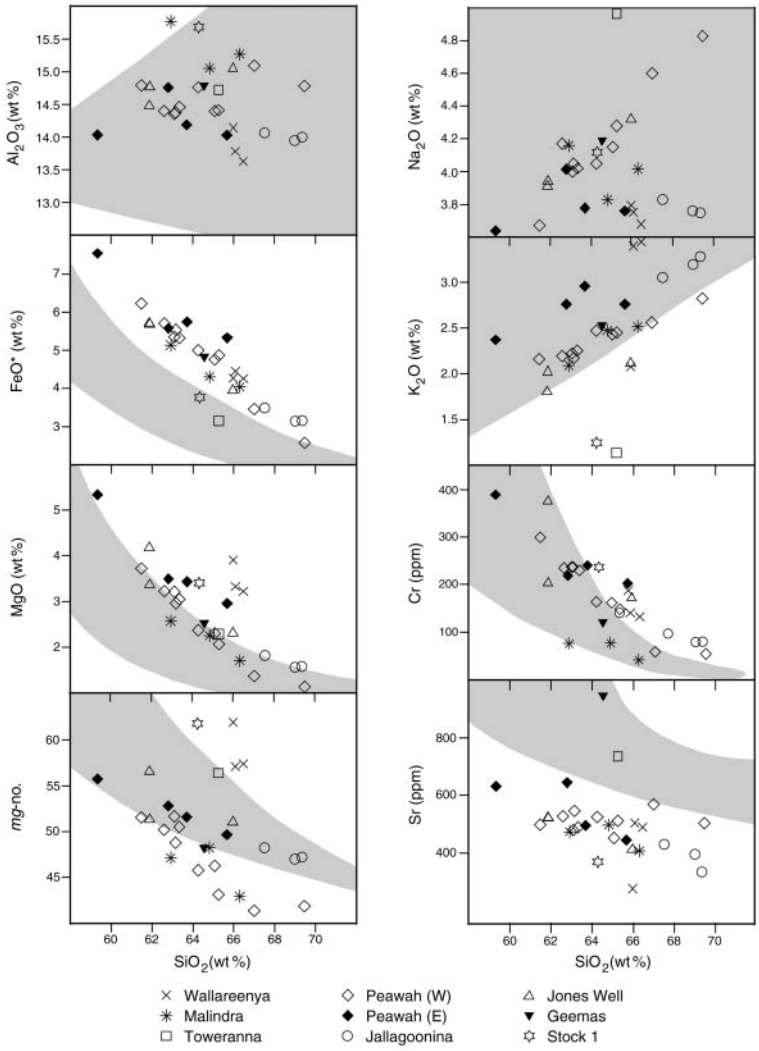

Fig. 2. Harker compositional variation diagrams showing selected major and trace element variations for rocks of the Pilbara high-Mg diorite suite. Shaded area shows the range for high-Mg diorite suites from the Archaean Superior Province of Canada (Stern *et al.*, 1989; Sutcliffe *et al.*, 1990; Stern & Hanson, 1991).

higher *mg*-number, MgO, Cr and Ni (Fig. 5). However, a single suite of TTG gneisses from the oldest (~3·45 Ga) part of the Shaw Granitoid Complex overlaps the low-MgO, -Cr, -Ni end of the range for the high-Mg diorite suite. In terms of these elements and the LILE, the TTG gneisses appear to form a compositional link between the high-Mg diorite series and TTG.

A SOURCE FOR HIGH-Mg DIORITES

The low *mg*-number of most crustal rocks suggests that they cannot be a source for high-Mg diorite. This is true even for the Archaean basalts of the Pilbara Craton, which have *mg*-number values between 42 and 61 [430 analyses from Glikson *et al.* (1986)] and commonly have concentrations of Cr and Ni that are only comparable with, or lower than, those of high-Mg diorite. A mantle source component is required to explain the high *mg*-number (≫62) and high Cr and Ni concentrations (Shirey & Hanson, 1984; Stern *et al.*, 1989; Stern & Hanson, 1991). Nevertheless, even the most primitive high-Mg diorite also shows extreme enrichments in LILE. The high *mg*-number, Cr and Ni suggest that LILE enrichments are not primarily the result of crystal fractionation. The high-Mg diorite suite is LILE rich and high field strength element (HFSE) depleted (Fig. 6), with many trace element ratios (high La/Yb, Th/Nb, Ba/Nb, La/Nb) similar to either Phanerozoic subduction-related magmas (e.g. Kay, 1980; Pearce, 1982) or to magmas contaminated

Table 2: Whole-rock analyses of the Pilbara high-Mg diorite suite

	1	2	3	4	5	6	7	8	9
Sample:	142257	142259	142260	142262	142306	118967	141965	141966	141967
Intrusion:	S1	JWS	JWS	JWS	G	PG(w)	PG(w)	PG(w)	PG(w)
Rock type:	gd	fgd	fgd	gd	gd	gd	gd	gd	gd
Lab.:	AGSO	AGSO	AGSO	AGSO	ANU	AGSO	AGSO	AGSO	AGSO
wt %									
SiO_2	64·22	61·88	61·86	65·95	64·54	61·47	64·25	63·15	63·09
TiO_2	0·39	0·56	0·51	0·39	0·53	0·57	0·51	0·54	0·55
Al_2O_3	15·68	14·77	14·48	15·05	14·79	14·79	14·76	14·38	14·35
Fe_2O_3*	4·17	6·31	6·34	4·39	5·37	6·92	5·56	6·15	5·95
MnO	0·06	0·09	0·08	0·06	0·08	0·07	0·07	0·07	0·07
MgO	3·41	3·36	4·17	2·31	2·53	3·72	2·37	2·96	3·21
CaO	4·81	4·83	4·67	3·53	3·19	4·67	3·71	4·18	4·31
Na_2O	4·12	3·94	3·91	4·32	4·19	3·67	4·05	4·05	4·00
K_2O	1·24	2·02	1·80	2·11	2·53	2·16	2·47	2·17	2·22
P_2O_5	0·13	0·28	0·24	0·16	0·24	0·27	0·28	0·32	0·29
LOI	1·86	2·02	2·00	1·66		2·07	1·63	1·67	1·75
Rest	0·18	0·29	0·26	0·25		0·33	0·29	0·29	0·29
Total	100·27	100·35	100·32	100·18	97·99	100·71	99·95	99·93	100·08
mg-no.	62	51	57	51	48	52	46	49	52
ppm									
Cs	7·9	5·4	8·6	7·4	4·9	5·0	9·3	16·1	9·7
Ba	441	808	695	700	1598	1067	1007	930	794
Rb	53	88	81	94	85	98	114	98	99
Sr	369	522	523	412	947	499	525	546	480
Pb	5·0	17·0	14·5	17·0	22·0	17·0	19·5	18·5	18·5
Th	5·0	11·2	9·3	10·2	13·4	8·1	12·3	9·3	11·1
U	1·0	2·6	3·3	2·3	2·6	1·7	3·0	1·9	3·0
Zr	98	136	130	122	141	155	166	150	151
Nb	3·7	6·3	5·3	5·1	7·0	6·7	7·4	6·7	6·7
Ta	<0·5	0·5	0·5	0·5		0·8	0·8	0·4	0·5
Y	9·4	18·5	15·2	10·9	16·0	15·0	13·3	13·8	14·6
Sc	13·0	14·0	12·0	8·0	11·0	11·0	9·5	10·0	12·0
V	85	106	98	63	71	99	78	90	88
Cr	136	116	215	98	67	170	94	135	135
Ni	64	56	99	49	17	89	41	54	59
Cu	24	40	30	20	6	28	35	19	37
Zn	46	75	73	58	66	78	76	77	81
Ga	16·9	17·7	17·0	17·2	18·0	16·6	18·7	18·5	18·2
La	17·8	47·4	39·7	34·6	53·0	47·1	54·5	50·8	46·7
Ce	32·3	93·3	76·7	62·4	108·0	90·0	102·9	96·0	91·7
Pr	3·5	10·7	8·6	6·5					
Nd	13·1	39·9	32·7	23·0	33·0	36·8	38·6	37·7	35·2
Sm	2·4	6·9	5·4	3·7		5·8	5·8	6·0	5·8
Eu	0·7	1·8	1·4	1·0		1·6	1·5	1·6	1·6
Gd	2·2	5·1	4·3	3·0		4·6	4·2	4·3	4·3
Tb	0·3	0·7	0·6	0·4		0·6	0·4	0·4	0·4
Dy	1·6	3·1	2·6	1·9		3·0	2·5	2·5	2·7
Ho	0·3	0·6	0·5	0·3		0·6	0·4	0·4	0·5
Er	0·8	1·6	1·3	0·9		1·6	1·2	1·2	1·3
Yb	0·8	1·4	1·2	0·9		1·3	1·0	1·0	1·1
Lu	0·1	0·2	0·2	0·1		0·2	0·1	0·1	0·2
La/Yb	22·25	33·86	33·08	38·44		36·23	54·50	50·80	42·45
$(La/Yb)_N$	14·88	22·64	22·12	25·71		24·23	36·44	33·97	28·39

	10	11	12	13	14	15	16	17	18	19
Sample:	141968	141969	141981	141927	141964	141971A	142346	142347	142348	142349
Intrusion:	PG(w)	PG(w)	PG(w)	PG(w)	PG(w)	PG(w)	PG(e)	PG(e)	PG(e)	PG(e)
Rock type:	gd	gd	gd	p	p	p	fgd	fgd	gd	gd
Lab.:	AGSO	AGSO	AGSO	AGSO	AGSO	AGSO	ANU	ANU	ANU	ANU
wt %										
SiO_2	65·06	62·59	66·99	69·46	65·26	63·33	62·80	59·33	63·70	65·66
TiO_2	0·44	0·56	0·43	0·34	0·44	0·55	0·55	0·63	0·55	0·49
Al_2O_3	14·40	14·40	15·09	14·78	14·41	14·46	14·76	14·03	14·19	14·03
Fe_2O_3*	5·29	6·34	3·85	2·86	5·41	5·91	6·19	8·38	6·38	5·92
MnO	0·06	0·07	0·04	0·03	0·07	0·07	0·08	0·11	0·08	0·07
MgO	2·30	3·23	1·37	1·04	2·07	3·05	3·50	5·33	3·43	2·95
CaO	3·54	4·39	3·02	2·31	3·58	4·19	4·34	5·49	3·42	3·56
Na_2O	4·15	4·17	4·60	4·83	4·28	4·02	4·01	3·64	3·78	3·76
K_2O	2·43	2·19	2·56	2·82	2·45	2·25	2·76	2·37	2·95	2·76
P_2O_5	0·23	0·29	0·21	0·15	0·23	0·28	0·34	0·43	0·23	0·24
LOI	1·74	1·49	1·58	0·97	1·65	1·65				
Rest	0·29	0·30	0·28	0·25	0·24	0·30				
Total	99·93	100·02	100·02	99·84	100·09	100·06	99·32	99·73	98·72	99·44
mg-no.	46	50	41	42	43	51	53	56	52	50
ppm										
Cs	11·2	7·2	2·6	4·1	9·7	8·2	2·8	2·7	1·1	0·4
Ba	834	850	1096	962	915	864	1194	1012	1174	1059
Rb	115	96	91	107	99	99	124	106	123	99
Sr	452	528	569	504	512	489	645	632	497	446
Pb	22·0	20·0	24·0	26·5	23·5	21·0	25·4	23·1	20·3	21·4
Th	12·4	9·7	12·6	13·2	11·9	10·9	15·0	13·0	13·0	18·0
U	3·4	1·5	4·9	3·7	3·2	1·5	2·0	3·0	2·0	2·0
Zr	156	150	177	187	158	163	164	145	147	139
Nb	6·8	6·5	7·0	6·7	6·5	7·0	8·4	8·3	8·4	8·2
Ta	0·6	0·5	0·7	0·6	0·5	0·5				
Y	12·0	14·6	10·9	8·3	11·8	14·8	17·4	19·8	15·5	14·6
Sc	9·0	13·5	6·5	4·0	7·5	11·0	12·0	14·0	14·0	10·0
V	66	94	51	31	61	91	84	104	82	68
Cr	90	134	30	28	78	131	124	224	136	114
Ni	41	62	16	14	33	57	66	120	66	54
Cu	23	39	10	13	22	19	8	40	14	16
Zn	70	80	67	63	67	81	70	79	70	61
Ga	18·0	18·7	20·8	20·6	17·4	18·1	17·2	17·5	17·1	16·3
La	48·4	46·3	53·6	47·7	47·4	49·0	58·6	61·6	32·8	57·2
Ce	90·1	90·2	105·5	87·5	89·3	95·8	119·0	130·2	71·2	107·2
Pr							20·4	14·9	16·3	15·0
Nd	31·4	35·4	36·7	29·8	32·7	36·7	58·4	63·7	41·1	43·4
Sm	5·0	6·0	5·5	4·4	5·0	6·1				
Eu	1·3	1·6	1·4	1·1	1·4	1·6				
Gd	3·5	4·3	3·6	2·8	3·5	4·4				
Tb	0·3	0·4	0·4	0·2	0·3	0·4				
Dy	2·2	2·8	2·1	1·6	2·1	2·7				
Ho	0·4	0·5	0·4	0·3	0·4	0·5				
Er	1·0	1·3	0·9	0·7	1·0	1·3				
Yb	0·9	1·1	0·7	0·6	0·9	1·1				
Lu	0·1	0·2	0·1		0·1	0·2				
La/Yb	53·78	42·09	76·57	79·50	52·67	44·55				
$(La/Yb)_N$	35·96	28·15	51·20	53·16	35·22	29·79				

Table 2: continued

	20	21	22	23	24	25	26	27	28	29
Sample:	141989	141990	141991	125025	9804-9146	9804-9147	9804-9149	9804-9159	9804-9163	9804-9194
Intrusion:	JS	JS	JS	T	MS	MS	MS	WG	WG	WG
Rock type:	gd	gd	gd	gd	gd	gd	gd	gd	gd	gd
Lab.:	AGSO	AGSO	AGSO	ANU	ANU	ANU	ANU	ANU	ANU	ANU
wt %										
SiO_2	68·99	69·34	67·51	65·25	66·29	62·91	64·81	66·07	66·46	65·96
TiO_2	0·41	0·41	0·47	0·36	0·55	0·64	0·58	0·41	0·38	0·41
Al_2O_3	13·95	14·00	14·07	14·72	15·27	15·77	15·06	13·78	13·63	14·14
Fe_2O_3*	3·51	3·52	3·89	3·51	4·49	5·71	4·79	4·94	4·73	4·75
MnO	0·05	0·05	0·05	0·06	0·07	0·08	0·07	0·08	0·07	0·07
MgO	1·57	1·59	1·83	2·29	1·71	2·57	2·25	3·33	3·22	3·90
CaO	2·44	1·99	2·77	3·50	3·76	4·55	4·27	3·06	2·94	3·14
Na_2O	3·76	3·75	3·83	4·98	4·02	4·16	3·83	3·75	3·68	3·79
K_2O	3·19	3·28	3·05	1·13	2·51	2·09	2·47	3·44	3·49	2·07
P_2O_5	0·19	0·17	0·20	0·19	0·20	0·28	0·25	0·17	0·16	0·12
LOI	1·66	1·55	1·71							
Total	99·72	99·65	99·38	95·99	98·87	98·75	98·38	99·04	98·77	98·36
mg-no.	47	47	48	56	43	47	48	57	57	62
ppm										
Cs	2·3	3·9	1·9	3·1	2·1	2·5	0·8	6·8	5·3	5·4
Ba	940	982	1506	1312	956	749	1081	1314	1276	512
Rb	100	114	99	36	90	86	98	134	136	92
Sr	397	335	431	735	408	474	498	505	490	277
Pb	30·0	29·5	27·0	24·8	30·1	22·7	26·5	31·4	31·2	17·8
Th	16·8	16·6	15·1	17·0	44·0	12·0	14·0	23·0	17·0	8·0
U	5·0	3·5	3·5	3·0	3·0	2·0	3·0	3·0	3·0	
Zr	157	154	162	139	143	154	139	137	133	116
Nb	10·0	9·4	9·5	5·7	8·7	8·0	9·2	7·5	6·8	7·5
Ta	1·0	1·1	1·0							
Y	16·5	15·8	16·5	13·9	17·4	17·3	17·0	15·9	15·0	14·6
Sc	6·5	5·5	7·0	10·0	10·0	10·0	10·0	10·0	10·0	10·0
V	48	48	56	56	68	90	80	66	60	62
Cr	44	44	54	82	22	42	42	154	152	192
Ni	21	21	24	32	18	32	30	52	56	90
Cu	16	15	17	14	20	18	22	16	12	14
Zn	49	48	53	55	60	65	61	49	51	52
Ga	18·2	17·6	18·4	16·7	17·6	18·2	17·5	15·4	15·7	17·1
La	48·7	50·2	54·5	61·1	47·3	42·2	57·4	57·7	48·0	19·6
Ce	101·3	102·7	110·3	109·1	94·0	87·8	110·2	103·9	85·7	39·0
Pr				25·4	13·6	9·7	16·0	16·5	15·2	6·8
Nd	37·7	38·2	39·6	48·4	41·1	42·0	50·6	45·4	41·5	16·9
Sm	6·0	5·8	6·2							
Eu	1·4	1·3	1·4							
Gd	4·2	4·1	4·3							
Tb	0·5	0·5	0·5							
Dy	2·8	2·7	2·9							
Ho	0·5	0·5	0·5							
Er	1·4	1·4	1·5							
Yb	1·3	1·2	1·4							
Lu	0·2	0·2	0·2							
La/Yb	37·46	41·83	38·93							
$(La/Yb)_N$	25·05	27·97	26·03							

*Total Fe reported as Fe^{3+}.
S1, Stock 1; JWS, Jones Well stock; G, Geemas; PG(w), Peawah Granodiorite (west); PG(e), Peawah Granodiorite (east); JS, Jallagoonina stock; T, Toweranna stock; MS, Malindra Well stock; WG, Wallareenya Granodiorite; gd, tonalite–granodiorite; fgd, fine-grained melanodiorite; p, plagioclase porphyry. For analytical details, see text.

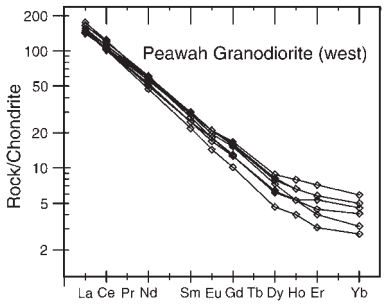

Fig. 3. Chondrite-normalized REE diagram for rocks of the Peawah Granodiorite (west) intrusion [normalization after Nakamura (1974)].

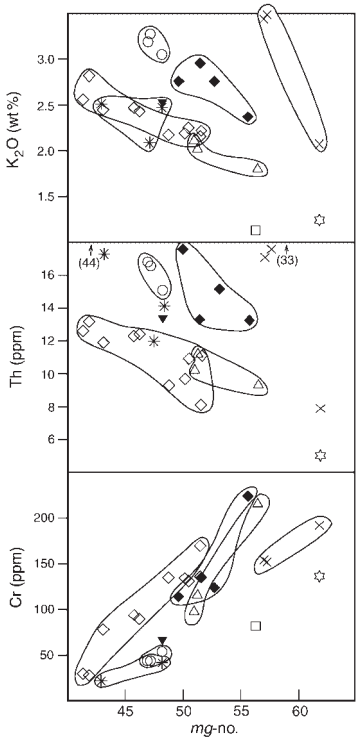

Fig. 4. Compositional variation diagrams plotting *mg*-number against K_2O, Th and Cr for rocks of the Pilbara high-Mg diorite suite. Fields have been drawn to aid in discrimination of various populations. Symbols as for Fig. 2.

by continental lithosphere (e.g. Cox & Hawkesworth, 1985).

Stern *et al.* (1989) used a range of compositions from basalt and komatiite to LILE-rich felsic crust to show that interaction between mafic to ultramafic melts and crustal material could not produce both the high Ni and Cr, and the high SiO_2 and LILE compositions of Superior Province high-Mg diorite. For the Pilbara high-Mg diorite suite, no mixing model can account for the fact that some of the most silica-rich intrusions, such as the Jallagoonina stock and Wallareenya granodiorite (Fig. 2), also have particularly high *mg*-numbers: one end-member in such models would require the unlikely combination of extremely high SiO_2 and *mg*-number. Negligible changes in Rb and Ba across the range of silica contents (or *mg*-number) also indicate that the high LILE content of the Pilbara high-Mg diorite cannot be a result of varying degrees of either magma mixing or assimilation of felsic crust. The most mafic rocks of the suite have Rb/Cs ratios around seven, similar to Archaean low Rb/Cs basalt and komatiite (<10; McDonough *et al.*, 1992). In contrast, present-day felsic crust has an Rb/Cs ratio of ~30 (Taylor & McLennan, 1985), and unless Archaean crust had a significantly lower ratio, it is unlikely that the high-Mg diorite incorporated a significant felsic component. In addition, rocks of the Pilbara high-Mg diorite suite show a virtual absence of inherited zircons (Nelson, 1996, 2000), further indicating very little crustal interaction. Consequently, the LILE-rich, HFSE-depleted nature of high-Mg diorite must reflect a mantle source component with similar characteristics.

COMPARISONS BETWEEN HIGH-Mg DIORITE AND PHANEROZOIC ROCKS

The close compositional similarity between high-Mg diorite and Cenozoic high-Mg andesite has long been recognized (e.g. Shirey & Hanson, 1984; Kelemen, 1995; Drummond *et al.*, 1996; Rapp, 1997). Yogodzinski *et al.* (1995) identified two types of high-Mg andesite from the Miocene to late Pleistocene western Aleutian arc, and called these rocks Adak-type and Piip-type. Adak-type high-Mg andesite crystallizes early clinopyroxene (but no olivine), has high La/Yb ratios, very high Sr (and other LILE), low HFSE (Table 1) and a mid-ocean ridge basalt (MORB)-like isotopic composition. These characteristics closely match those of Cenozoic adakite, which is thought to be restricted to zones where young, hot, oceanic crust is subducted and partially melted at pressures high enough to stabilize garnet ± amphibole (eclogite to garnet amphibolite facies) (e.g. Defant & Drummond, 1990). However, the *mg*-number and concentrations of Cr, Ni and MgO are significantly higher in Adak-type high-Mg andesite than in most adakites (Table 1). Accordingly, Yogodzinski *et al.* (1995), proposed that Adak-type high-Mg andesite is the result of contamination of adakite by mantle peridotite (e.g. Kay, 1978; Kelemen *et al.*, 1993; Sen & Dunn, 1994) (i.e. a 'wedge-modified' adakite). This process essentially involves assimilation of peridotite and crystallization of orthopyroxene (Yogodzinski *et al.*, 1995), or garnet and orthopyroxene (Rapp *et al.*, 1999). Rapp *et al.* (1999) showed experimentally that wedge-modified adakite would not only preserve typical adakite

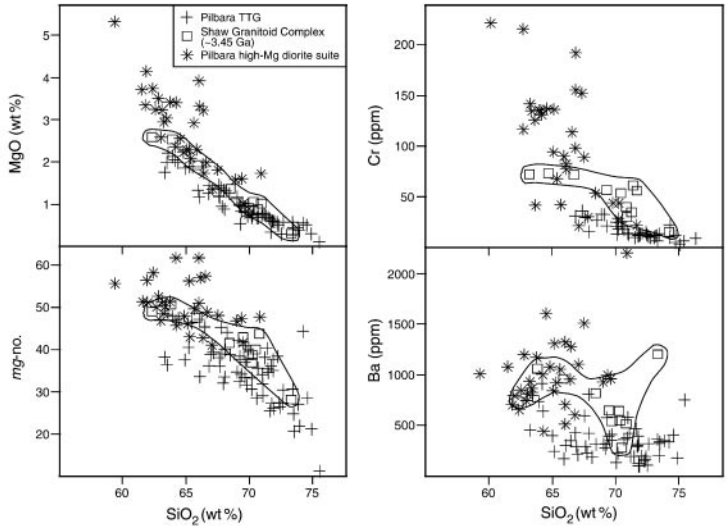

Fig. 5. Harker compositional variation diagrams comparing selected major and trace element concentrations for rocks of the Pilbara high-Mg diorite suite with those for ~3·45 Ga TTG from the Shaw Granitoid Complex [data from Bickle *et al.* (1983, 1993)], and other (generally >3·44 Ga) TTG from the eastern granite–greenstone terrain of the Pilbara Craton [data from Collins (1993), W. Collins (unpublished data, 1983), the Australian Geological Survey Organisation (unpublished data, 1998, 1999) and the Geological Survey of Western Australia (unpublished data, 1998, 1999)]. Data for the ~3·45 Ga TTG from the Shaw Granitoid Complex are enclosed by a continuous line and exclude those from rocks described by Bickle *et al.* (1983, 1989, 1993) as magmatically layered.

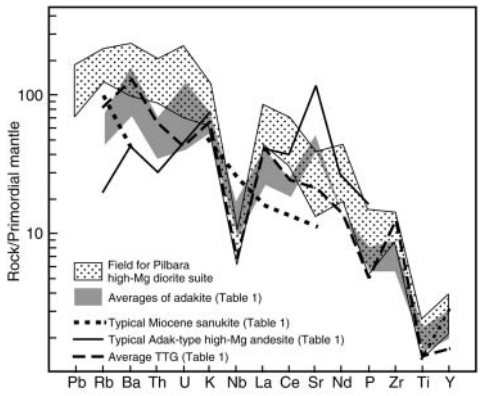

Fig. 6. Primordial mantle normalized spider diagram comparing incompatible trace-element concentration patterns for all rocks of the Pilbara high-Mg diorite suite with representative or average compositions of high-Mg andesite and adakite from Table 1 [normalization after Sun & McDonough (1989)].

trace element ratios, but would show uniform increases in trace element concentrations, through consumption of melt during the contamination process.

The second type of high-Mg andesite identified by Yogodzinski *et al.* (1995), the Piip-type, crystallizes early olivine, and compared with wedge-modified adakite, generally has higher MgO, *mg*-number, Ni and Cr, lower K_2O and Sr (LILE), and much lower La/Yb ratios (Table 1). These rocks are thought to be derived via direct melting of peridotitic mantle that was enriched in LILE through addition of either a slab-derived melt (i.e. adakite) or volatile phase. Alternatively, Yogodzinski & Kelemen (1998) suggested Piip-type melts may result when wedge-modified adakite mixes, in the mantle wedge, with arc basalt. Whichever is the case, wedge-modified adakite and Piip-type high-Mg andesite differ primarily in terms of the degree to which a slab-derived component contributes to magma genesis.

Yogodzinski *et al.* (1995) noted that Miocene high-Mg andesite (sanukite) of Japan is typical of the Piip-type, consistent with experimental evidence suggesting that sanukite could be derived via melting of mantle peridotite under hydrous conditions (Tatsumi & Ishizaka, 1982). Shirey & Hanson (1984) recognized geochemical similarities between Miocene sanukite and Archaean high-Mg diorite (Table 1) and argued for a similar origin for high-Mg diorite. Apart from high *mg*-number, Cr and Ni, these rocks have similarly high concentrations of HREE, with Yb generally >1·0 ppm and commonly >1·6 ppm. Yogodzinski *et al.* (1995), however, pointed out that La/Yb ratios in high-Mg diorite (67–77) are much higher than in Miocene sanukite (5–11) or in other Piip-type rocks (4–6), and are more like those of adakite (19–65) and wedge-modified adakite (~45) (Table 1 and Fig. 7). High-Mg diorite also has generally lower *mg*-number and K_2O, and significantly higher Sr and LREE than sanukite and other Piip-type rocks, and in these regards is more like wedge-modified adakite (Table 1 and Fig. 6). The implication here is that melting of basaltic crust was significantly more important in the

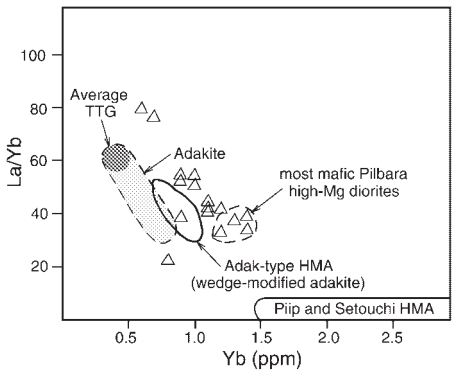

Fig. 7. Plots of La/Yb vs Yb comparing rocks of the Peawah Granodiorite (Pilbara high-Mg diorite suite) with average TTG [from Martin (1994)], average adakite [field encloses averages from both Defant *et al.* (1991) and Drummond *et al.* (1996)], Adak-type high-Mg andesite (HMA) (Yogodzinski *et al.*, 1995) and Piip-type HMA, including Miocene sanukite from the Japanese Setouchi volcanic belt (Tatsumi & Ishizaka, 1982; Yogodzinski *et al.*, 1995).

derivation of high-Mg diorite than is suggested by analogies to sanukite, and that the tectonic setting and petrogenetic models proposed for wedge-modified adakite may also be relevant to high-Mg diorite.

PETROGENETIC LINKS BETWEEN ADAKITE, TTG AND HIGH-Mg DIORITE

Adakite is relatively rare in the Cenozoic, but rocks with similar major and trace element compositions form a major component of the voluminous Archaean TTG series (Table 1 and Figs 6 and 7). It is widely accepted that TTG also result from melting of basaltic material at pressures high enough to stabilize garnet ± amphibole, producing tonalitic melts with characteristically high La/Yb and Sr/Y ratios (e.g. Barker & Arth, 1976; Barker, 1979; Tarney *et al.*, 1979; Martin, 1986, 1999; Drummond & Defant, 1990; Beard & Lofgren, 1991; Rapp *et al.*, 1991; Rapp, 1997). There is also wide acceptance that some form of plate tectonics was active in the Archaean (e.g. Hoffman, 1989; Card, 1990; De Wit *et al.*, 1992; Kröner & Layer, 1992; Lowe & Ernst, 1992; Lowe, 1997; De Wit, 1998; but see Hamilton, 1995). It seems reasonable, therefore, to suggest that TTG may have formed in a subduction environment, and is an Archaean analogue of Cenozoic adakite (e.g. Drummond & Defant, 1990; Drummond *et al.*, 1996; Rapp, 1997; Martin, 1999).

Wedge-modified adakites are subduction-related Cenozoic rocks with compositions very similar to Archaean high-Mg diorite. It is possible, therefore, that high-Mg diorite is an Archaean analogue of wedge-modified adakite, formed as TTG, derived via partial melting of subducted oceanic crust, interacted with the peridotitic mantle wedge (e.g. Yogodzinski *et al.*, 1995; Drummond *et al.*, 1996; Rapp, 1997).

However, none of the few reported occurrences of high-Mg diorite appears to directly relate to either subduction or TTG magmatism. Rather, intrusion appears to have been late-kinematic (e.g. Evans & Hanson, 1997) or post-kinematic (Davis *et al.*, 1994) and there is a strong temporal and spatial link between at least some high-Mg diorite suites and generally sodic, felsic, alkali magmatism [e.g. Otto Stock Syenite of the Superior Province (Sutcliffe *et al.*, 1990); Portree Granitoid Complex of the Pilbara Craton]. This fundamental difference in setting between high-Mg diorite and wedge-modified adakite shows that if a relationship exists between high-Mg diorite and subduction magmatism, including TTG, it is not via a single-stage process.

It is possible, however, that high-Mg diorite results from the remelting of a TTG–mantle hybrid source and this may also explain why high-Mg diorite has LILE concentrations that are at least as high as, and Yb concentrations that are higher than, those of TTG. Figure 8 shows that the LILE and REE concentrations of the Pilbara high-Mg diorites can be successfully modelled as a high-degree (~25%) partial (batch) melt of a hybrid source produced by mixing ~40% TTG–adakite into peridotite. Melting under garnet-free conditions, leaving an orthopyroxene-rich residue, reproduces the characteristically high HREE, whereas high La/Yb ratios are a combined result of remelting a source already LREE enriched through a significant TTG component.

If high-Mg diorite is a result of any form (single or two stage) of TTG and melt–mantle interaction, a subduction origin for TTG is required. Although such an origin is commonly favoured for TTG (e.g. Drummond & Defant, 1990; Drummond *et al.*, 1996; Rapp, 1997; Martin, 1999), Atherton & Petford (1993) and Petford & Atherton (1996) showed that hydrous basaltic material, underplating a thick crustal root, can also partially melt to produce adakite (TTG)-like rock. Martin (1986) also showed that steeper geotherms meant that the *P–T* requirements for TTG production may have been commonly attained in the Archaean. Consequently, the tectonic setting of TTG genesis needs to be carefully considered.

Beard *et al.* (1993) pointed out that melt derived from a subducted slab should show clear evidence of having equilibrated, or reacted, with the mantle wedge through which it ascends. This appears to be the case for most adakite suites from subduction environments, which either comprise, or include, low-silica (<65 wt %) and high-*mg*-number (>47 and commonly >50) (Fig. 9), high-Cr and -Ni rocks (e.g. Defant *et al.*, 1991; Mahlburg Kay *et al.*, 1993; Sajona *et al.*, 1994; Stern & Kilian, 1996). A small number of TTG suites also contain rocks with low

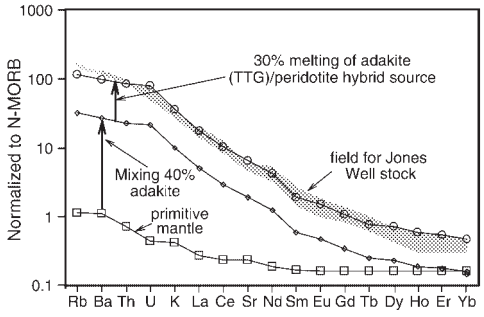

Fig. 8. Plot comparing the LILE and REE concentrations of the most mafic rocks of the Pilbara high-Mg diorite suite (melanodiorite from the Jones Well stock) with hypothetical melts modelled by mixing ~40% adakite into peridotite [using primitive mantle compositions from Sun & McDonough (1989)], followed by ~30% batch melting, leaving a residual containing ~90% orthopyroxene and 10% clinopyroxene. Partition coefficient data for clinopyroxene and orthopyroxene are from a variety of sources; REE data from Arth (1976), Frey *et al.* (1978) and A. Ewart [unpublished data (1987), cited by Sheraton & Simons (1992)], other elements are from Frey *et al.* (1978), Pearce & Norry (1979), Green *et al.* (1989) and A. Ewart [unpublished data (1987), cited by Sheraton & Simons (1992)]. For Th and U partition coefficients of zero were arbitrarily used. (Note, as average Cenozoic adakite and Archaean TTG appear to have significantly different Sr/Ba, modelled Ba, Sr and K values were taken from average TTG from the eastern granite–greenstone terrain of the Pilbara Craton.)

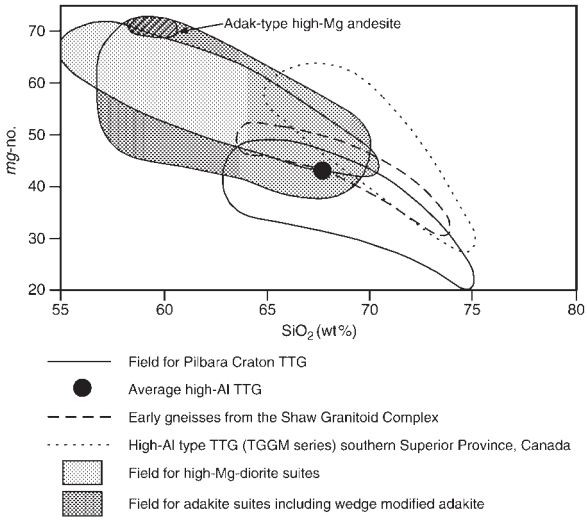

Fig. 9. Compositional variation diagram of *mg*-number vs SiO_2, showing the fields for TTG from the Pilbara Craton [from Bickle *et al.* (1983, 1989, 1993), W. Collins (unpublished data, 1983), Collins (1993), the Australian Geological Survey Organisation (unpublished data, 1998, 1999) and the Geological Survey of Western Australia (unpublished data, 1998, 1999)], early gneisses from the Shaw Granitoid Complex (Bickle *et al.*, 1983, 1989, 1993), TTG from the southern Superior Province [TGGM series of Feng & Kerrich (1992)], Pilbara and Superior high-Mg diorite suites (Stern *et al.*, 1989; Sutcliffe *et al.*, 1990; Stern & Hanson, 1991; this publication), adakite suites, including wedge-modified adakite (Defant *et al.*, 1991; Mahlburg Kay *et al.*, 1993; Sajona *et al.*, 1994; Morris, 1995; Yogodzinski *et al.*, 1995; Stern & Killian, 1996 and average TTG (Martin, 1994). Most Archaean TTG suites lie within the field defined by TTG from the Pilbara Craton.

silica (< ~65 wt %), reasonably high *mg*-number (between 47 and 50), and high Ni and Cr concentrations (Fig. 9). Such suites include the gneisses from the Shaw Granitoid Complex of the eastern Pilbara Craton (Bickle *et al.*, 1983, 1989, 1993) and high-Al TTG from the southern Superior Province of Canada (Feng & Kerrich, 1992). However, average TTG has considerably lower *mg*-numbers, and lower Ni and Cr concentrations (Table 1), and the compositional range for most TTG suites is limited to the higher silica, lower *mg*-number end of the range for adakite and wedge-modified adakite (Fig. 9). If the trends to higher *mg*-number and lower SiO_2 shown by Cenozoic adakite suites reflect the incorporation of a mantle component, then many (most?) TTG suites show no clear evidence of that component. Such suites, therefore, are either not subduction related or have somehow avoided contamination within the mantle wedge. The latter would seem thermodynamically improbable, as the mantle wedge should be hotter than either the subducting slab or the adakite melt. In addition, Rapp *et al.* (1999) showed that under experimental conditions, small amounts of contamination (~10% peridotite) produce large (~20%) changes in *mg*-number. Only TTG that interacted with mantle peridotite can have been the precursor to high-Mg magmatism, whether by a single- or two-stage process. If subduction-derived TTG suites are rare, then this would explain why high-Mg diorite magmatism is also rare.

Regardless of how high-Mg diorites form, the scarcity of these rocks itself suggests that the required conditions were not met during all felsic crust-forming events, in all Archaean terrains. In the section below, we propose that Archaean high-Mg diorite results through the remelting of a mantle source region, extensively hybridized or metasomatized through the interaction of peridotite with a felsic (TTG-like) melt. We base this selection of source components on the close compositional analogies between high-Mg diorite and wedge-modified adakite, but we invoke a two-stage (remelting) process based mainly on the post-kinematic setting of the Pilbara high-Mg diorite suite.

TECTONIC MODELS FOR HIGH-Mg DIORITE AND TTG

Some TTG suites, like those from southern Superior Province of North America and possibly the gneisses from the Shaw Granitoid Complex, show evidence of mantle interaction (high-*mg*-number, low-SiO_2 TTG suites; Fig. 9). However, the compositions of many (most?) suites, including the majority from the Pilbara Craton, appear more consistent with melting of hydrous basaltic material at the base of the Archaean crust and under a

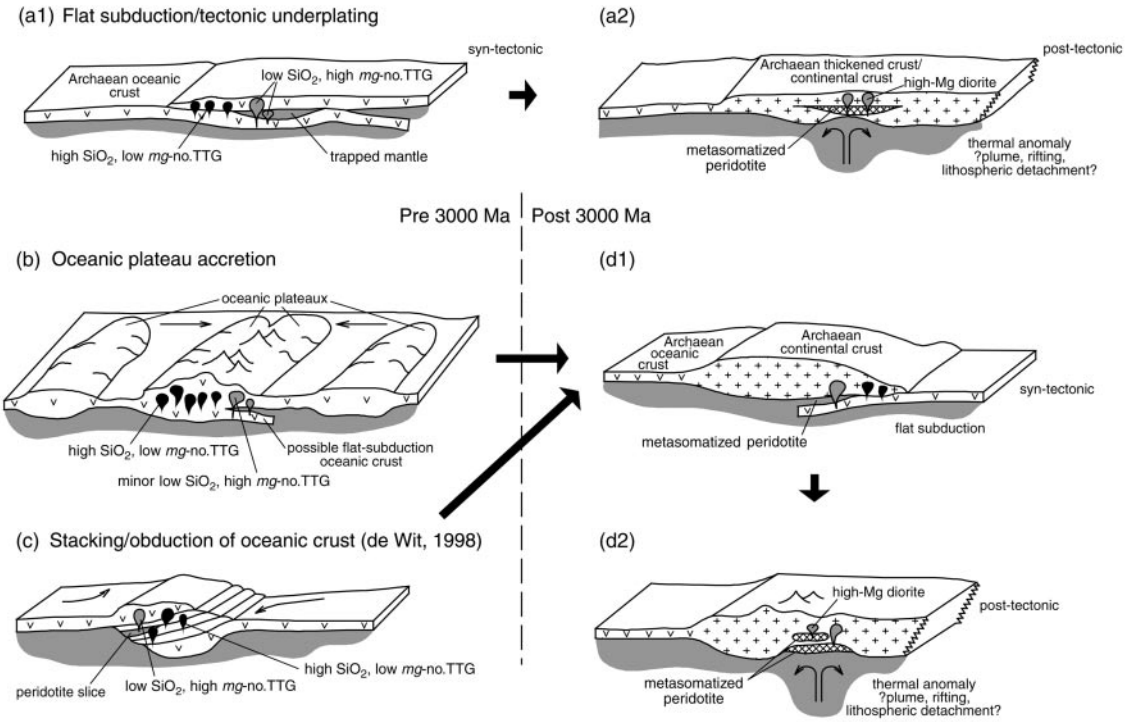

Fig. 10. Schematic representation of possible integrated tectonic models for TTG and high-Mg diorite genesis.

typical Archaean geotherm (low-*mg*-number, high-SiO_2 TTG suites; Fig. 9). One way to accommodate such compositional variation is if subduction during the Archaean was extremely flat, or approximated underthrusting, and locally excluded the mantle wedge (i.e. a tectonic underplate; Fig. 10, a1). Flat subduction of rapidly moving, young, thick and buoyant Archaean oceanic crust has been advocated as a significant mode of Archaean subduction by Abbott & Hoffman (1984) and Abbott (1991). Flat subduction of oceanic crust, or possibly oceanic plateaux (e.g. Tarney & Jones, 1994), may have produced TTG melts, many of which may have ascended without encountering a mantle wedge. Other TTG melts (e.g. gneisses from the Shaw Granitoid Complex and TTG from the southern Superior Province; Fig. 9) passed through, and interacted with, peridotite in a thin mantle wedge.

During reaction with mantle wedge peridotite, small-volume TTG melts would be totally consumed (e.g. Rapp *et al.*, 1999), leaving a strongly hybridized or metasomatized mantle. According to Kepezhinskas *et al.* (1996), strongly metasomatized pyroxenite xenoliths in basalt from the northern section of the Kamchatka arc contain both a mineral assemblage matching products of experimental reactions between felsic melt and ultramafic rock, and dacitic veins broadly comparable in composition with adakite. This hybrid mantle may form the source for high-Mg diorite during a later melting event (Fig. 10, a2).

Alternatively, if melting of a lower, hydrous, basaltic portion of a thick Archaean crust is the primary mechanism of TTG genesis, then processes involving sequential stacking, or obduction, of buoyant oceanic crust (De Wit, 1998) and/or successive accretion of thick, buoyant, oceanic plateaux (e.g. Desrochers *et al.*, 1993; Condie, 1997) might be more appropriate models of early Archaean crustal growth than subduction (Fig. 10b and c).

Sen & Dunn (1994) and Tarney & Jones (1994) noted that partial melts of oceanic basalt are depleted in Sr and Ba compared with either TTG or adakite. These deficiencies may be overcome if spilitized alkali- (Sr, Ba)-rich basalt is the source (e.g. Rapp *et al.*, 1999), and it is also likely that the slab source for many adakites includes LILE-rich oceanic sediment (e.g. Stern & Kilian, 1996). Modern ocean plateau basalts commonly have trace element concentrations between those of mid-ocean ridge basalt and ocean island basalt (Weis *et al.*, 1989; Richards *et al.*, 1991; Lassiter *et al.*, 1995; Kerr *et al.*, 1997; Neal *et al.*, 1997), with high Sr and Ba concentrations. Tarney & Jones (1994) noted that Archaean oceanic plateau basalts may also provide a suitable source for TTG.

An alternative to a flat-subduction and tectonic underplating model for TTG and high-Mg diorite magmatism begins with thick ($> \sim 35$ km; Martin, 1986) crust formed

by stacking of locally spilitized oceanic crust and/or by of accretion of oceanic plateaux. If crustal thickening is rapid, the appropriate conditions (eclogite facies) for partial melting can be achieved before the crust dehydrates, and low-*mg*-number, high-SiO_2 TTG suites should result (Fig. 10b and c). High-Mg diorite suites, and high-*mg*-number, low-SiO_2 TTG suites, which require a mantle source component, may relate to possible (flat) subduction events during accretion of oceanic plateaux. An interesting feature of the documented high-Mg diorite suites is that they form late, not simply in terms of a given tectonic cycle, but in terms of the overall evolution of a given Archaean province, and all are younger than ~3000 Ma. Therefore, it is possible that high-Mg diorite magmatism, or at least the subduction event that produced its hybridized mantle source, heralds a transition from early Archaean tectonic styles dominated by oceanic plate stacking and plateau accretion, to a period where subduction of the cooler, thinner and less buoyant oceanic crust became a more viable process (Fig. 10d1 and d2).

LATE ARCHAEAN EVOLUTION OF THE PILBARA CRATON

In addition to the broader tectonic significance of high-Mg diorite magmatism, intrusion of the Pilbara high-Mg diorite suite also provides some of the most important clues to the Late Archaean evolution of the Pilbara granite–greenstone terrain. In the central part of the terrain, Pb isotopic ages were reset during a significant tectonothermal event at ~2950 Ma (Oversby, 1976). Intrusion of the Pilbara high-Mg diorite suite and the alkaline Portree Granitoid Complex represents virtually the entire known extent of magmatism at that time, and both are restricted to the Mallina Basin (Fig. 1). The mantle-derived high-Mg diorite suite intruded along major extensional basin faults. Within less than 10 my, large volumes of monzogranite and syenogranite, of crustal origin (Champion & Smithies, 1998), swamped the central Pilbara region. These are most voluminous adjacent to the Mallina Basin, and from the available geochronology (Nelson, 1997, 1998, 1999), show a clear progressive decrease in age away from the basin towards the southeast.

De Wit (1998) and Beakhouse *et al.* (1999) speculated that high-Mg diorite magmatism occurs during late extensional collapse of an Archaean province. In the case of the Pilbara high-Mg diorite suite, we suggest that the restriction of ~2950 Ma magmatism to the Mallina Basin and the concentration of ~2940–2930 Ma monzogranite and syenogranite magmatism adjacent to the same region, with a seemingly systematic decrease in both age and volume away from the region, points to a process more localized than regional extensional collapse. It seems more likely that mantle upwelling beneath the central Pilbara Craton, possibly caused by either local lithospheric detachment–delamination or a mantle plume, remobilized a mantle source region, previously hybridized during a subduction event, to produce high-Mg diorite magmatism. At the same time, high-temperature melting of a metasomatized basal crust produced the sodic alkaline granite of the Portree Granitoid Complex, and inductive heating of the lower- to middle-crustal region caused partial melting and production of monzogranite and syenogranite magmas.

CONCLUSIONS

The ~2950 Ma Pilbara high-Mg diorite suite intrudes the youngest supracrustal sequences of the central part of the Pilbara granite–greenstone terrain, in a post-kinematic setting associated with alkaline magmatism but not with TTG magmatism. The rocks are broadly similar in composition to the ~2700 Ma high-Mg diorite suites of the Superior Province and have distinctly higher *mg*-number and Cr and Ni concentrations than TTG, at equivalent silica contents. High LILE concentrations cannot be explained through crustal contamination of a mafic magma, and together with high *mg*-number and Cr and Ni concentrations indicate an LILE-enriched mantle source.

TTG shows compositional similarities to felsic partial melts of subducted, young, hot, basaltic crust (adakite), and it is commonly suggested that TTG may likewise be subduction related. High-Mg diorite is compositionally very similar to Cenozoic high-*mg*-number adakite (wedge-modified adakite), thought to result when adakite is contaminated by peridotite during ascent through the mantle wedge. However, the late- to post-kinematic setting of high-Mg diorite excludes a similar origin. The close compositional similarities between wedge-modified adakite and high-Mg diorite can be explained by a two-stage model whereby high-Mg diorite results from the remelting of a mantle source region, previously hybridized by the addition of significant amounts of a subduction-derived TTG-like melt.

However, the lack of such evidence as rocks with high *mg*-number and low SiO_2 contents for interaction between many TTG melts and mantle peridotite indicates that the amount of TTG derived via subduction may be limited. This would explain why high-Mg diorite magmatism is rare compared with TTG magmatism on a global Archaean scale. Melting of hydrated basaltic material at the base of thickened crust (e.g. Atherton & Petford, 1993; Petford & Atherton, 1996), may be a more appropriate model for most TTG.

Tectonic models that incorporate tectonic underplating of oceanic crust, sequential stacking, or obduction, of

oceanic crust (De Wit, 1998) and/or successive accretion of oceanic plateaux (e.g. Desrochers *et al.*, 1993; Condie, 1997) predict TTG generation mainly at the base of thickened crust and might be more appropriate models of early Archaean crustal growth than modern-style subduction and arc accretion. High-Mg diorite magmatism may herald a transition from early Archaean tectonic styles dominated by tectonic underplating, oceanic plate stacking and plateau accretion, to a period where cooler, thinner and less buoyant oceanic crust allowed processes more akin to modern-style subduction and arc accretion.

ACKNOWLEDGEMENTS

This work has benefited greatly through numerous discussions with Arthur Hickman, Paul Morris, Steve Sheppard, Shen-su Sun and Martin Van Kranendonk, and through reviews by Michael Atherton, Kevin Cassidy, Suzanne Mahlburg Kay, Paul Morris, Steve Sheppard, Shen-su Sun and Marjorie Wilson. We thank S. Dowsett, L. Cosgrove, T. Edwards and P. Carroll for drafting of figures. This work is published with the permission of the Director, Geological Survey of Western Australia, and the Executive Director, Australian Geological Survey Organisation.

REFERENCES

Abbott D. (1991). The case for accretion of the tectosphere by buoyant subduction. *Geophysical Research Letters* **18**(4), 585–588.

Abbott, D. H. & Hoffman, S. E. (1984). Archaean plate tectonics revisited. 1. Heat flow, spreading rate, and the age of subducting oceanic lithosphere and their effects on the origin and the evolution of continents. *Tectonics* **3**(4), 429–448.

Arth, J. G. (1976). Behaviour of trace elements during magmatic processes—a summary of theoretical models and their applications. *Journal of Research of the US Geological Survey* **4**, 41–47.

Arth, J. G. & Hanson, G. N. (1975). Geochemistry and origin of the Early Precambrian crust of north-eastern Minnesota. *Geochimica et Cosmochimica Acta* **39**, 325–362.

Atherton, M. P. & Petford, N. (1993). Generation of sodium-rich magmas from newly underplated basaltic crust. *Nature* **362**, 144–146.

Barker, F. (1979). Trondhjemite: definition, environment and hypotheses of origin. In: Barker, F. (ed.) *Trondhjemites, Dacites, and Related Rocks.* Amsterdam: Elsevier, pp. 1–12.

Barker, F. & Arth, J. G. (1976). Generation of trondjhemitic–tonalitic liquids and Archaean bimodal trondhjemite–basalt suites. *Geology* **4**, 596–600.

Beakhouse, G. P., Heaman, L. M. & Creaser, R. A. (1999). Geochemical and U–Pb zircon geochronological constraints on the development of a Late Archean greenstone belt at Birch Lake, Superior Province, Canada. *Precambrian Research* **97**, 77–97.

Beard, J. S. & Lofgren, G. E. (1991). Dehydration melting and water-saturated melting of basaltic and andesitic greenstones and amphibolites at 1, 3, and 6·9 kbar. *Journal of Petrology* **32**, 365–461.

Beard, J. S., Bergantz, G. W., Defant, M. J. & Drummond, M. S. (1993). Origin and emplacement of low-K silicic magmas in subduction setting. *Penrose Conference Report. GSA Today* **3**, 38.

Bickle, M. J., Bettenay, L. F., Barley, M. E., Groves, D. I., Chapman, H. J., Campbell, I. H. & de Laeter, J. R. (1983). A 3500 Ma plutonic and volcanic calc-alkaline province in the Archaean east Pilbara Block. *Contributions to Mineralogy and Petrology* **84**, 25–35.

Bickle, M. J., Bettenay, L. F., Chapman, H. J., Groves, D. I., McNaughton, N. J., Campbell, I. H. & de Laeter, J. R. (1989). The age and origin of the younger granitic plutons of the Shaw Batholith in the Archaean Pilbara Block, western Australia. *Contributions to Mineralogy and Petrology* **101**, 361–376.

Bickle, M. J., Bettenay, L. F., Chapman, H. J., Groves, D. I., McNaughton, N. J., Campbell, I. H. & de Laeter, J. R. (1993). Origin of the 3500–3300 Ma calc-alkaline rocks in the Pilbara Archaean: isotopic and geochemical constraints from the Shaw batholith. *Precambrian Research* **60**, 117–149.

Card, K. D. (1990). A review of the Superior Province of the Canadian Shield, a product of Archean accretion. *Precambrian Research* **48**, 99–156.

Champion, D. C. & Smithies, H. (1998). Archaean granites of the Yilgarn and Pilbara Cratons. *The Bruce Chappell Symposium: Granites, Island Arcs, the Mantle and Ore Deposits, Abstract Volume. Australian Geological Survey Organisation Record* **1998/33**, 24–25.

Collins, W. J. (1983). Geological evolution of an Archaean batholith. Ph.D. dissertation, La Trobe University, Melbourne, Vic.

Collins, W. J. (1993). Melting of Archaean sialic crust under high $a H_2O$ conditions: genesis of 3300 Ma Na-rich granitoids in the Mount Edgar Batholith, Pilbara Block, Western Australia. *Precambrian Research* **60**, 151–174.

Condie, K. C. (1997). Contrasting sources for upper and lower continental crust: the greenstone connection. *Journal of Geology* **105**, 729–736.

Cox, K. G. & Hawkesworth, C. J. (1985). Relative contribution of crust and mantle to flood basalt volcanism, Mahabaleshwar area, Deccan Traps. *Philosophical Transactions of the Royal Society of London, Series A* **310**, 627–641.

Davis, W. J., Fryer, B. J. & King, J. E. (1994). Geochemistry and Late Archean plutonism and its significance to the tectonic development of the Slave craton. *Precambrian Research* **67**, 207–241.

Defant, M. J. & Drummond, M. S. (1990). Derivation of some modern arc magmas by melting of young subducted lithosphere. *Nature* **347**, 662–665.

Defant, M. J., Richerson, P. M., de Boer, J. Z., Stewart, R. H., Maury, R. C., Bellon, H., Drummond, M. S., Feigenson, M. D. & Jackson, T. E. (1991). Dacite genesis via slab melting and differentiation: petrogenesis of La Yeguada Volcanic Complex, Panama. *Journal of Petrology* **32**, 1101–1142.

Desrochers, J.-P., Hubert, C., Ludden, J. & Pilote, P. (1993). Accretion of Archean oceanic plateau fragments in the Abitibi greenstone belt, Canada. *Geology* **21**, 451–454.

De Wit, M. J. (1998). On Archean granites, greenstones, cratons and tectonics: does the evidence demand a verdict? *Precambrian Research* **91**, 181–226.

De Wit, M. J., Roering, C., Hart, R. J., Armstrong, R. A., de Ronde, C. E. J., Green, R. W. E., Tredoux, M., Peberdy, E. & Hart, R. A. (1992). Formation of an Archaean continent. *Nature* **357**, 553–562.

Drummond, M. S. & Defant, M. J. (1990). A model for trondhjemite–tonalite–dacite genesis and crustal growth via slab melting: Archaean to modern comparisons. *Journal of Geophysical Research* **95B**, 21503–21521.

Drummond, M. S., Defant, M. J. & Kepezhinskas, P. K. (1996). Petrogenesis of slab-derived trondhjemite–tonalite–dacite/adakite magmas. *Transactions of the Royal Society of Edinburgh: Earth Sciences* **87**, 205–215.

Eggins, S. M., Woodhead, J. D., Kinsley, L. P. J., Mortimer, G. E., Sylvester, P., McCulloch, M. T., Hergt, J. M. & Handler, M. R. (1997). A simple method for the precise determination of >40 trace elements in geological samples by ICPMS using enriched isotope internal standardisation. *Chemical Geology* **134**, 311–326.

Evans, O. C. & Hanson, G. N. (1997). Late- to post-kinematic Archean granitoids of the S.W. Superior Province: derivation through direct mantle melting. In: de Wit, M. J. & Ashwal, L. D. (eds) *Greenstone Belts*. Oxford: Oxford University Press, pp. 280–295.

Feng, R. & Kerrich, R. (1992). Geochemical evolution of granitoids from the Archaean Abitibi Southern Volcanic Zone and the Pontiac subprovince, Superior Province, Canada: implications for tectonic history and source regions. *Chemical Geology* **98**, 23–70.

Frey, F. A., Green, D. H. & Roy, S. D., (1978). Integrated models of basalt petrogenesis: a study of quartz tholeiites to olivine melilitites from south eastern Australia utilizing geochemical and experimental petrological data. *Journal of Petrology* **19**, 463–513.

Glikson, A. Y., Davy, R. & Hickman, A. H. (1986). Geochemical data files of Archaean volcanic rocks, Pilbara Block, Western Australia. *BMR Record* **1986/14**, 2 pp.

Green, T. H., Sie, S. H., Ryan, C. G. & Cousens, D. R., (1989). Proton microprobe-determined partitioning of Nb, Ta, Sr, and Y between garnet, clinopyroxene and basaltic magma at high pressure and temperature. *Chemical Geology* **74**, 201–216.

Hamilton, W. B. (1995). Subduction systems and magmatism. In: Smellie, J. L. (ed.) *Volcanism Associated with Extension at Consuming Plate Margins. Geological Society, London, Special Publications* **81**, 3–28.

Hoffman, P. F. (1989). Precambrian geology and tectonic history of North America. In: Bally, A. W. & Palmer, A. R. (eds) *The Geology of North America—an Overview. The Geology of North America, A*. Boulder, CO: Geological Society of America, pp. 447–512.

Kay, R. W. (1978). Aleutian magnesian andesite: melts from subducted Pacific ocean crust. *Journal of Volcanology and Geothermal Research* **4**, 117–132.

Kay, R. W. (1980). Volcanic arc magma genesis: implications for element recycling in the crust–upper mantle system. *Journal of Geology* **88**, 497–522.

Kelemen, P. B. (1995). Genesis of high Mg# andesites and the continental crust. *Contributions to Mineralogy and Petrology* **120**, 1–19.

Kelemen, B. P., Shimizu, N. & Dunn, T. (1993). Relative depletion of niobium in some arc magmas and the continental crust: partitioning of K, Nb, La and Ce during melt/rock reaction in the upper mantle. *Earth and Planetary Science Letters* **120**, 111–134.

Kepezhinskas, P. K., Defant, M. J. & Drummond, M. S. (1996). Progressive enrichment of island arc mantle by melt–peridotite interaction inferred from Kamchatka xenolites. *Geochimica et Cosmochimica Acta* **60**, 1217–1229.

Kerr, A. C., Tarney, J., Marriner, G. F., Nivia, A. & Saunders, A. D. (1997). The Caribbean–Colombian Cretaceous igneous province: the internal anatomy of an oceanic plateau. In: Mahoney, J. J. & Coffin, M. (eds) *Large Igneous Provinces: Continental, Oceanic, and Planetary Flood Volcanism. Geophysical Monograph, American Geophysical Union* **100**, 123–144.

Kröner, A. & Layer, P. W. (1992). Crust formation and plate motion in the early Archean. *Science* **256**, 1405–1411.

Lassiter, J. C., DePaolo, D. J. & Mahoney, J. J. (1995). Geochemistry of the Wrangellia flood basalt province: implications for the role of continental and oceanic lithosphere in flood basalt genesis. *Journal of Petrology* **36**, 983–997.

Lowe, D. R. (1997). Archean greenstone-related sedimentary rocks. In: de Wit, M. J. & Ashwal, L. D. (eds) *Greenstone Belts*. Oxford: Oxford University Press, pp. 121–169.

Lowe, D. R. & Ernst, W. G. (1992). The Archean geologic record. In: Schopf, J. W. & Klein, C. (eds) *The Proterozoic Biosphere*. Cambridge: Cambridge University Press, pp. 13–19.

Mahlburg Kay, S., Ramos, V. A. & Marquez, M. (1993). Evidence in Cerro Pampa volcanic rocks for slab-melting prior to ridge–trench collision in southern South America. *Journal of Geology* **101**, 703–714.

Martin, H. (1986). Effect of steeper Archaean geothermal gradient on geochemistry of subduction-zone magmas. *Geology* **14**, 753–756.

Martin, H. (1994). The Archean grey gneisses and the genesis of continental crust. In: Condie, K. C. (ed.) *Archean Crustal Evolution*. Amsterdam: Elsevier, pp. 205–259.

Martin, H. (1999). Adakitic magmas: modern analogues of Archaean granitoids. *Lithos* **46**, 411–429.

McDonough, W. F., Sun, S.-S., Ringwood, A. E., Jagoutz, E. & Hofmann, A. W. (1992). Potassium, rubidium, and cesium in the Earth and Moon and the evolution of the mantle of the Earth. *Geochimica et Cosmochimica Acta* **56**, 1001–1012.

Morris, P. A. (1995). Slab melting as an explanation of Quaternary volcanism and aseismicity in southwest Japan. *Geology* **23**, 395–398.

Nakamura, N. (1974). Determination of REE, Ba, Mg, Na and K in carbonaceous and ordinary chondrites. *Geochimica et Cosmochimica Acta* **38**, 757–775.

Neal, C. R., Mahoney, J. J., Kroenke, L. W., Duncan, R. A. & Petterson, M. G. (1997). The Ontong Java Platean. In: Mahoney, J. J. & Coffin, M. (eds) *Large Igneous Provinces: Continental, Oceanic, and Planetary Flood Volcanism. Geophysical Monograph, American Geophysical Union* **100**, 183–216.

Nelson, D. R. (1996). Compilation of SHRIMP U–Pb zircon geochronology data, 1995. *Geological Survey of Western Australia Record* **1996/2**, 150 pp.

Nelson, D. R. (1997). Compilation of SHRIMP U–Pb zircon geochronology data, 1996. *Geological Survey of Western Australia Record* **1997/2**, 189 pp.

Nelson, D. R. (1998). Compilation of SHRIMP U–Pb zircon geochronology data, 1997. *Geological Survey of Western Australia Record* **1998/2**, 242 pp.

Nelson, D. R. (1999). Compilation of SHRIMP U–Pb zircon geochronology data, 1998. *Geological Survey of Western Australia Record* **1999/2**, 222 pp.

Nelson, D. R. (2000). Compilation of SHRIMP U–Pb zircon geochronology data, 1999. *Geological Survey of Western Australia Record* **2000/2** (in press).

Norrish, K. & Chappell, B. W. (1977). X-ray fluorescence spectrometry. In: Zussman, J. (ed.) *Physical Methods in Determinative Mineralogy*, 2nd edn. London: Academic Press, pp. 201–272.

Norrish, K. & Hutton, J. T. (1969). An accurate X-ray spectrographic method for the analysis of a wide range of geological samples. *Geochimica et Cosmochimica Acta* **33**, 431–453.

Oversby, V. M. (1976). Isotopic ages and geochemistry of Archaean acid igneous rocks from the Pilbara, Western Australia. *Geochimica et Cosmochimica Acta* **40**, 817–829.

Pearce, J. A. (1982). Trace element characteristics of lavas from destructive plate boundaries. In: Thorpe, R. S. (ed.) *Andesites: Orogenic Andesites and Related Rocks*. Chichester: Wiley, pp. 525–548.

Pearce, J. A. & Norry, M. J., (1979). Petrogenetic implications of Ti, Zr, Y and Nb variations in volcanic rocks. *Contributions to Mineralogy and Petrology* **69**, 33–47.

Petford, N. & Atherton, M. (1996). Na-rich partial melts from newly underplated basaltic crust: the Cordillera Blanca batholith, Peru. *Journal of Petrology* **37**, 1491–1521.

Rapp, R. P. (1997). Heterogeneous source regions for Archean granitoids. In: de Wit, M. J. & Ashwal, L. D. (eds) *Greenstone Belts*. Oxford: Oxford University Press, pp. 267–279.

Rapp, P. R., Watson, E. B. & Miller, C. F. (1991). Partial melting of amphibolite/eclogite and the origin of Archean trondhjemites and tonalites. *Precambrian Research* **51**, 1–25.

Rapp, P. R., Shimizu, N., Norman, M. D. & Applegate, G. S. (1999). Reaction between slab-derived melts and peridotite in the mantle wedge: experimental constraints at 3·8 GPa. *Chemical Geology* **160**, 335–356.

Richards, M. A., Jones, D. L., Duncan, R. A. & DePaolo, D. J. (1991). A mantle plume initiation model for the Wrangellia flood basalt and other oceanic plateaus. *Science* **254**, 263–267.

Sajona, F. G., Bellon, H., Maury, R. C., Pubellier, M., Cotton, J. & Rangin, C. (1994). Magmatic response to abrupt changes in geodynamic setting: Pliocene–Quaternary calc-alkaline and Nb-enriched lavas from Mindanao (Philippines). *Tectonophysics* **237**, 47–72.

Sen, C. & Dunn, T. (1994). Dehydration melting of a basaltic composition amphibolite at 1·5 and 2·0 GPa: implications for the origin of adakite. *Contributions to Mineralogy and Petrology* **117**, 394–409.

Shapiro, L. & Brannock, W. W. (1962). Rapid analysis of silicate, carbonate and phosphate rocks. *US Geological Survey Bulletin* **1144-A**, 56 pp.

Sheraton, J. W. & Simons, L. (1992). Geochemical data analysis system (GDA) reference manual. *Australian Geological Survey Organisation Record* **1992/1**, 183 pp.

Shirey, S. B. & Hanson, G. N. (1984). Mantle-derived Archaean monzodiorites and trachyandesites. *Nature* **310**, 222–224.

Smithies, R. H. (1998). *Geology of the Mount Wohler 1:100 000 sheet.* 1:100 000 Geological Series Explanatory Notes. Perth: Western Australia Geological Survey, 19 pp.

Smithies, R. H. & Champion, D. C. (1998). Secular compositional changes in Archaean granitoid rocks of the west Pilbara. *Western Australia Geological Survey, Annual Review 1997–98*, 71–76.

Smithies, R. H., Hickman, A. H. & Nelson, D. R. (1999). New constraints on the evolution of the Mallina Basin, and their bearing on relationships between the contrasting eastern and western granite–greenstone terranes of the Archaean Pilbara Craton, Western Australia. *Precambrian Research* **94**, 11–28.

Stern, C. R. & Kilian, R. (1996). Role of the subducted slab, mantle wedge and continental crust in the generation of adakites from the Andean Austral Volcanic Zone. *Contributions to Mineralogy and Petrology* **123**, 263–281.

Stern, R. A. & Hanson, G. N. (1991). Archean high-Mg granodiorite: a derivative of light rare earth element-enriched monzodiorite of mantle origin. *Journal of Petrology* **32**, 201–238.

Stern, R. A., Hanson, G. N. & Shirey, S. B. (1989). Petrogenesis of mantle-derived, LILE-enriched Archean monzodiorites and trachyandesites (sanukitoids) in southwestern Superior Province. *Canadian Journal of Earth Sciences* **26**, 1688–1712.

Sun, S.-S. & McDonough, W. F. (1989). Chemical and isotopic systematics of oceanic basalts: implications for mantle compositions and processes. *In*: Saunders, A. D. & Norry, M. J. (eds) *Magmatism in Ocean Basins. Geological Society, London, Special Publications* **42**, 313–345.

Sutcliffe, R. H., Smith, A. R., Doherty, W. & Barnett, R. L. (1990). Mantle derivation of Archaean amphibole-bearing granitoid and associated mafic rocks: evidence from the southern Superior Province, Canada. *Contributions to Mineralogy and Petrology* **105**, 255–274.

Tarney, J. & Jones, C. E. (1994). Trace element geochemistry of orogenic igneous rocks and crustal growth models. *Journal of the Geological Society, London* **151**, 855–868.

Tarney, J., Weaver, B. L. & Drury, S. A. (1979). Geochemistry of Archaean trondhjemitic and tonalitic gneisses from Scotland and E. Greenland. In: Barker, F. (ed.) *Trondhjemites, Dacites and Related Rocks*. Amsterdam: Elsevier, pp. 275–299.

Tatsumi, Y. & Ishizaka, K. (1982). Origin of high-magnesian andesite in the Setouchi volcanic belt, southwest Japan, I. Petrological and chemical characteristics. *Earth and Planetary Science Letters* **60**, 293–304.

Taylor, S. R. & McLennan, S. M. (1985). *The Continental Crust: its Composition and Evolution*. Oxford: Blackwell.

Weis, D., Bassias, Y., Gautier, I. & Mennessier, J.-P. (1989). Dupal anomaly in existence 115 Ma ago: evidence from isotopic study of the Kerguelen Plateau (South Indian Ocean). *Geochimica et Cosmochimica Acta* **53**, 2125–2131.

Wells, P. R. A. (1977). Pyroxene thermometry in simple and complex systems. *Contributions to Mineralogy and Petrology* **62**, 129–139.

Yogodzinski, G. M. & Kelemen, P. B. (1998). Slab melting in the Aleutians: implications of an ion probe study of clinopyroxene in primitive adakite and basalt. *Earth and Planetary Science Letters* **158**, 53–65.

Yogodzinski, G. M., Kay, R. W., Volynets, O. N., Koloskov, A. V. & Kay, S. M. (1995). Magnesian andesite in the western Aleutian Komandorsky region: implications for slab melting and processes in the mantle wedge. *Geological Society of America Bulletin* **107**(5), 505–519.